Published online 26 September 2006 *Nucleic Acids Research, 2006, Vol. 34, No. 18* ***5217–5231***
doi:10.1093/nar/gkl677

Human RECQ5β helicase promotes strand exchange on synthetic DNA structures resembling a stalled replication fork

Radhakrishnan Kanagaraj, Nurten Saydam, Patrick L. Garcia, Lu Zheng and Pavel Janscak*

Institute of Molecular Cancer Research, University of Zurich, Winterthurerstrasse 190, CH-8057 Zurich, Switzerland

Received July 25, 2006; Revised August 30, 2006; Accepted September 4, 2006

ABSTRACT

The role of the human RECQ5β helicase in the maintenance of genomic stability remains elusive. Here we show that RECQ5β promotes strand exchange between arms of synthetic forked DNA structures resembling a stalled replication fork in a reaction dependent on ATP hydrolysis. BLM and WRN can also promote strand exchange on these structures. However, in the presence of human replication protein A (hRPA), the action of these RecQ-type helicases is strongly biased towards unwinding of the parental duplex, an effect not seen with RECQ5β. A domain within the non-conserved portion of RECQ5β is identified as being important for its ability to unwind the lagging-strand arm and to promote strand exchange on hRPA-coated forked structures. We also show that RECQ5β associates with DNA replication factories in S phase nuclei and persists at the sites of stalled replication forks after exposure of cells to UV irradiation. Moreover, RECQ5β is found to physically interact with the polymerase processivity factor proliferating cell nuclear antigen *in vitro* and *in vivo*. Collectively, these findings suggest that RECQ5β may promote regression of stalled replication forks to facilitate the bypass of replication-blocking lesions by template-switching. Loss of such activity could explain the elevated level of mitotic crossovers observed in RECQ5β-deficient cells.

INTRODUCTION

The progression of DNA replication forks is frequently impaired by DNA damage, particularly if the blocking lesion is located on the leading-strand template (1). In this case, synthesis of the leading strand is halted at the lesion, while the lagging-strand synthesis continues beyond the lesion site, resulting in a fork structure with an extensive gap in the leading strand (2,3). Replication fork stalling poses a serious threat to genomic stability because it can trigger unscheduled DNA recombination events and hence lead to gross chromosomal re-arrangements that can induce tumorigenesis (4,5). To avoid these detrimental consequences of DNA replication arrest, cells can switch to different DNA damage bypass modes that permit replication across the lesion (1,3,6,7). One of these mechanisms is proposed to involve a transient template switch to the undamaged sister chromatid, allowing the replicative polymerase to synthesize the sequence complementary to the blocking lesion in an error-free manner (8). It is believed that such template-switching is achieved by a movement of the fork backward so as to re-anneal the original template strands and displace the newly synthesized strands which themselves anneal to generate a Holliday junction structure with a short arm (1). Indeed, such structures have been observed to accumulate upon replication arrest both in prokaryotic and in eukaryotic cells (8–11). However, it is not clear whether the formation of these structures is promoted enzymatically or occurs spontaneously.

Proteins belonging to the RecQ family of 3′–5′ DNA helicases are implicated in the processing of aberrant DNA structures arising during DNA replication and repair (12). Defects in three of the five known human RecQ homologues have been found to be associated with different autosomal recessive disorders characterized by genomic instability and cancer predisposition—mutations in BLM, WRN and RECQ4 give rise to Bloom syndrome, Werner syndrome and Rothmund–Thomson syndrome, respectively (12). BLM is known to suppress crossovers during homologous recombination (HR) presumably through its unique ability to act in conjunction with DNA topoisomerase IIIα to decatenate recombination intermediates containing double Holliday junctions (13). WRN promotes lagging-strand replication of G-rich telomeric regions and resolves telomeric D-loops in a manner regulated by the TRF1 and TRF2 proteins (14,15). RECQ4 is proposed to be important for the initiation of DNA replication by promoting the loading of replication protein A on unwound origins (16).

The role of the human RECQ5 protein in the maintenance of genomic stability remains to be elucidated. The inactivation

*To whom correspondence should be addressed. Tel: +41 44 635 3470; Fax: +41 44 635 3484; Email: pjanscak@imcr.unizh.ch

of the *Recq5* gene in mouse embryonic stem cells results in a significant increase in the frequency of sister chromatid exchanges (SCEs) comparable to that caused by *Blm* gene inactivation (17). Deletion of both *Recq5* and *Blm* genes leads to an even higher frequency of SCEs compared to the single mutants, suggesting that BLM and RECQ5 operate in different pathways that suppress mitotic recombination (17). In contrast to the other human RecQ homologues, RECQ5 exists in at least three different isoforms resulting from alternative mRNA splicing (18). The largest splice variant, RECQ5β functions not only as a 3′–5′ DNA helicase, but also possesses an intrinsic DNA strand-annealing activity residing in the unique C-terminal half of the protein (19). This strand-annealing activity is suppressed if the helicase is in its ATP-bound state, suggesting that RECQ5β may mediate DNA transactions that require a coordinated action of helicase and strand-annealing activities, such as replication fork regression.

Here we show that the RECQ5β helicase has the ability to promote strand exchange between arms of synthetic forked DNA structures that resemble a stalled replication fork in a reaction stimulated by the human replication protein A (hRPA). In contrast, hRPA is found to block strand exchange by BLM and WRN by driving these helicases to mediate unwinding of the parental duplex. On forked DNA structures with heterologous arms, RECQ5β preferentially unwinds the lagging-strand duplex, whereas BLM and WRN show a strong preference for unwinding of the parental duplex even in the absence of hRPA. The ability of RECQ5β to catalyze the lagging-strand unwinding and strand exchange on hRPA-coated forked structures is dependent on a short region located within the non-conserved portion of RECQ5β. In addition, we show by immunofluorescence microscopy that RECQ5β localizes to DNA replication factories in S phase nuclei and persists at the sites of stalled replication forks. Moreover, we have found that RECQ5β physically interacts with the polymerase processivity factor proliferating cell nuclear antigen (PCNA) *in vivo* and *in vitro*. Based on these findings, we propose that RECQ5β could mediate regression of stalled replication forks to facilitate DNA damage bypass by template-switching.

MATERIALS AND METHODS

Plasmid constructions and protein purifications

The bacterial expression vectors for the RECQ5β fragments encompassing the amino acid residues 1–774 (pPG13) and 542–991 (pPG14), fused to the C-terminus of glutathione-*S*-transferase (GST), were constructed by PCR amplification of the corresponding regions of the RECQ5β cDNA and their insertion in pGEX-2TK between the EcoRI and BamHI sites. The bacterial vectors expressing $RECQ5^{1–725}$ (pPG18), $RECQ5^{1–651}$ (pPG20), $RECQ5^{1–561}$ (pPG21) and $RECQ5^{1–475}$ (pPG19) as C-terminal fusions with a self-cleaving tag including chitin-binding domain (CBD) were constructed in the same way as the vector for the full-size RECQ5β (19). The BamHI–NcoI fragment of BLM cDNA in pcDNA3 (20), and the NcoI–XhoI fragment of pJK1 (21), including the remaining part of the BLM coding sequence fused C-terminally to a His_6 tag, were cloned in pFastBac1 via BamHI and XhoI sites to yield the plasmid pZL4, which was used to generate a bacmid for the expression of BLM in Sf9 cells by the means of baculovirus system.

The RECQ5β protein and its variants were produced in bacteria and purified as described previously (19). His-tagged BLM was produced in Sf9 by the means of baculovirus system and purified on a 5 ml HighTrap Chelating (Ni^{2+}) column under previously described conditions (21). To increase the purity, the BLM protein was further loaded on to a 1 ml MonoQ column equilibrated with buffer containing 50 mM Tris (pH 7.5), 10% (v/v) glycerol, 200 mM NaCl and 0.1 mM EDTA, and eluted with a linear concentration gradient of NaCl (200–650 mM). WRN, hRPA and PCNA were prepared essentially as described (22–24). *Escherichia coli* single-strand DNA-binding protein was purchased from Promega.

Antibodies

An antibody against the C-terminal fragment of RECQ5β encompassing amino acids 675–991 was raised in rabbit (Clonestar Ltd, Czech Republic) and purified on a RECQ5β-Sepharose 4A column.

DNA substrates

All oligonucleotides used for the preparation of DNA substrates were purchased PAGE-purified from Microsynth (Switzerland). The sequences of the oligonucleotides (RK1-7) and the schemes of DNA substrates are shown in Supplementary Table 1. Where required, oligonucleotides were labeled at the 5′ end with T4 polynucleotide kinase (NEB) and [γ-^{32}P]ATP using standard procedure. The oligonucleotides were annealed under conditions described previously (25).

Strand exchange and helicase assays

Reactions were carried out at 37°C in buffer HA containing 20 mM Tris–acetate (pH 7.9), 50 mM KOAc, 10 mM $Mg(OAc)_2$, 1 mM DTT and 50 μg/ml BSA. Where required, $Mg(OAc)_2$ concentration was varied in the range from 0 to 10 mM. For the strand exchange assays, 1 nM RK1/RK2 partial duplex was incubated with 40 nM RECQ5β and either 1 nM RK3 oligonucleotide or 1 nM RK3/RK4 partial duplex in a volume of 100 μl of buffer HA to generate forked DNA structures depicted in Figures 1A and 2A, respectively. After 10 min, ATP was added to a final concentration of 2 mM. Aliquots (5 μl) were removed at different reaction time points (both before and after the addition of ATP) and analyzed. In the control experiment, ATP was substituted with ATPγS (2 mM). The 3′-flap duplex for strand-exchange assays with BLM (10 nM) and WRN (5 nM) was pre-formed by the spontaneous annealing of the constituent oligonucleotides RK1, RK2 and RK3, with the RK2 oligonucleotide being present in a 5-fold molar excess over the others. Helicase reactions were carried out as described previously (19). Where required, hRPA (20 nM) was added to DNA 1 min before the addition of RecQ proteins and ATP. All reactions were terminated by adding 0.5 reaction volumes of solution S (150 mM EDTA, 2% SDS, 30% glycerol and 0.1% bromophenol blue) and

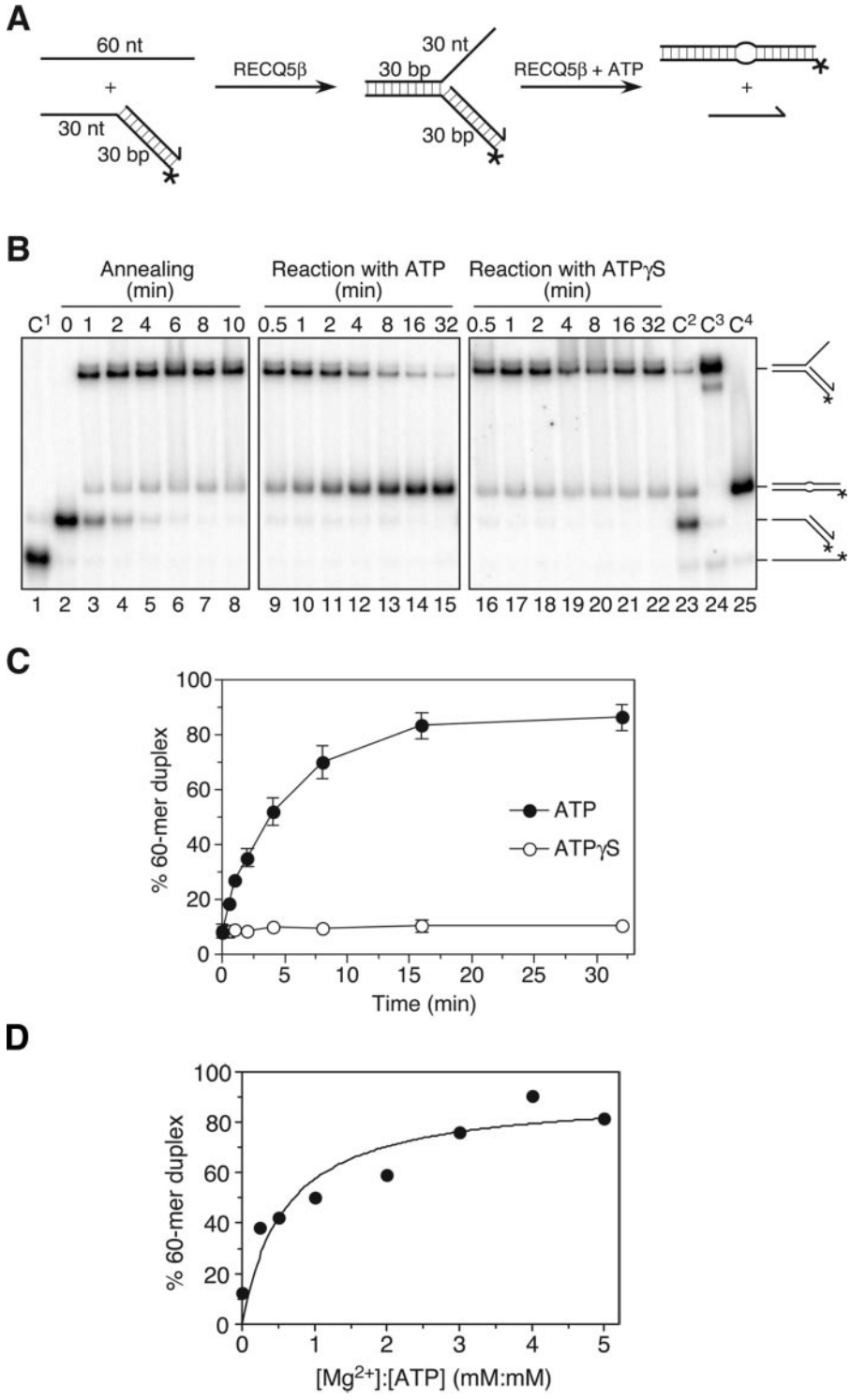

Figure 1. Strand-exchange by RECQ5β on synthetic forked DNA structure with homologous arms lacking the leading strand. (**A**) Scheme of the assay. The lengths of individual arms are indicated in nucleotides (nt) or base pairs (bp). The 3′ end of the lagging oligonucleotide is indicated by an arrow and the position of the 5′-^{32}P label is marked by an asterisk. The homologous leading and lagging arms have a 5 nt heterology at the fork junction to prevent spontaneous strand exchange. (**B**) 1 nM ^{32}P-labeled 30mer/60mer duplex (RK1/RK2) was incubated with 1 nM 60mer complementary oligonucleotide (RK3) in the presence of 40 nM RECQ5β to form the forked DNA structure. After 10 min, either ATP or ATPγS were added to a final concentration of 2 mM. Aliquots from different reaction time points, before and after addition of the nucleotide, were analyzed by non-denaturing PAGE followed by phosphorimaging. C^1–C^4, markers for the DNA substrate and the reaction products. (**C**) Quantification of the ATP and ATPγS containing reactions. Relative concentration of the 60mer duplex product is plotted versus reaction time. The data points represent the average values from three independent experiments. (**D**) Dependence of the strand-exchange activity of RECQ5β on Mg^{2+} ion concentration. Reaction mixtures contained 1 nM 3′-flap DNA substrate, 40 nM RECQ5β and 2 mM ATP with increasing concentrations of $Mg(OAc)_2$. Relative concentration of the 60mer duplex product after 32 min was measured as in (B) and (C). The lines drawn are only to guide the eye.

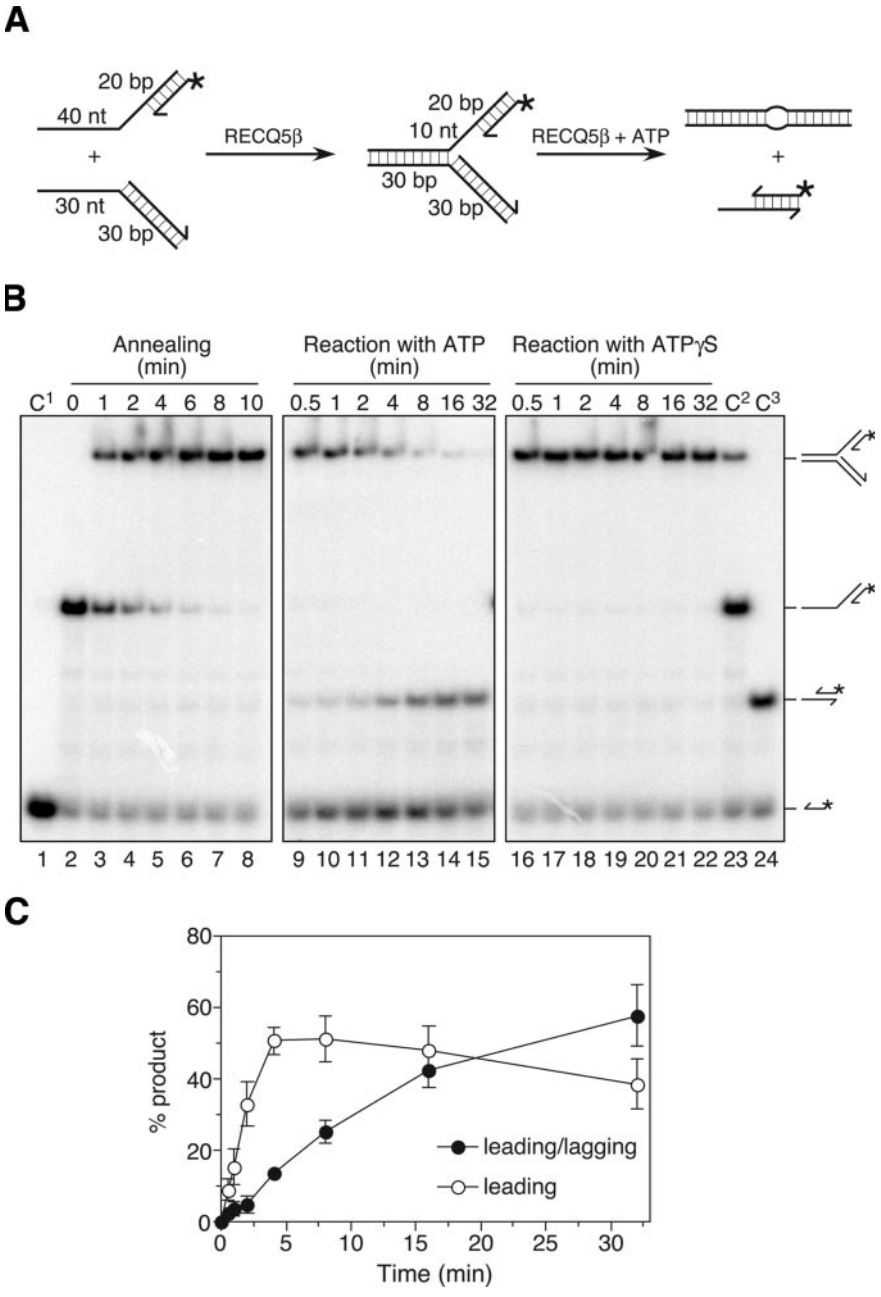

Figure 2. Strand-exchange by RECQ5β on synthetic forked DNA duplex with a leading-strand gap. (**A**) Scheme of the assay. The oligonucleotides used are the same as in Figure 1, except for an additional 20mer representing the leading strand. (**B**) 1 nM ^{32}P-labeled 20mer/60mer duplex (RK1/RK2) was incubated with 1 nM 30mer/60mer duplex (RK3/RK4) in the presence of 40 nM RECQ5β to form the forked DNA structure. After 10 min, either ATP or ATPγS were added to a final concentration of 2 mM. Aliquots of the annealing and the nucleotide-driven reactions were analyzed by non-denaturing PAGE. C^1–C^3, markers for the DNA substrate and the reaction products. (**C**) Quantification of the ATP- driven reaction. The relative concentrations of the unwound 20mer oligonucleotide (leading strand; open circles) and subsequently formed 20mer/30mer partial duplex (leading/lagging duplex; closed circles) are plotted versus reaction time. The data points represent the average values from three independent experiments.

subsequently treated with proteinase K (0.1 mg/ml) at 37°C for 10 min. The reaction mixtures were resolved by electrophoresis in a 10% (w/v) non-denaturing polyacrylamide gel (PAGE; acrylamide/bis-acrylamide 19:1). Radiolabeled DNA species were visualized by autoradiography and quantified using a Molecular Dynamics Typhoon 9400 scanner with associated IMAGEQUANT software. The relative concentration of radiolabeled products was expressed as percentage of total DNA.

Strand annealing assays

Strand annealing activity of RECQ5β and its deletion variants was measured using complementary 50mer oligonucleotides as described previously (19).

Cell culture

All the cell lines used in this study were maintained in DMEM (OmniLab) supplemented with 10% fetal calf

serum (Life Technologies) and streptomycin/penicillin (100 U/ml). To prepare synchronized population of cells, cultures at ~60% confluency were treated with 2 mM hydroxyurea (HU) for 16 h. UV treatments (at a dose of 20 J/m^2) were carried out in a UV-Stratalinker 1800 equipped with a 254 nm UV lamp (Stratagene). Where required, *cis*-diamminedichloro-platinum (CDDP) was added to a final concentration of 20 μM. For cell cycle analyses, ethanol-fixed cells were stained with propidium iodide (20 μg/ml; Molecular Probes) and subjected to flow cytometry in a Becton Dickinson cell sorter.

Immunofluorescence assays

Cells grown on cover slips were fixed in methanol for 30 min at −20°C, which was followed by incubation in acetone for 30 s. After blocking in PBS supplemented with 3% low-fat milk (blocking solution), cover slips were incubated overnight at 4°C with primary antibodies [rabbit polyclonal anti-RECQ5β (this study; 1:800) and mouse monoclonal anti-PCNA (PC-10, Santa Cruz; 1:200); all antibodies were diluted in blocking solution]. After washing with PBS, the cells were incubated with FITC-conjugated sheep anti-rabbit (Sigma; 1:700) and Texas Red-conjugated donkey anti-mouse (Abcam; 1:200) secondary antibodies for 1 h at 37°C. The nuclei were then counterstained with DAPI (0.1 μg/ml; Sigma) for 10 min, washed with water and mounted in SlowFade Antifade reagent (Molecular Probes). Images were captured by Olympus IX81 fluorescence microscope. At least 150 nuclei were analyzed in each experiment.

Immunoprecipitation assays

Cells were subjected to trypsinization, harvested by centrifugation and resuspended in lysis buffer [50 mM Tris–HCl, pH 8.0, 120 mM NaCl and 0.5% (v/v) NP-40] supplemented with protease inhibitor cocktail (Complete, Mini; Roche). After a 30 min incubation on ice, the lysate was treated with 10 U of RNase-free DNase I (Roche) at 25°C for 30 min, and clarified by centrifugation. The protein extracts (1 mg) were incubated overnight at 4°C with purified rabbit anti-RECQ5β IgGs (1 μg) or with IgGs purified from pre-immune serum (1 μg). Immune complexes were subsequently incubated with protein A/G–agarose beads (20 μl, Amersham Biosciences) for 1 h at 4°C. Immunoprecipitates were analyzed by western blotting.

GST/CBD pull-down assays

GST- and CBD-tagged fragments of RECQ5β were produced in *E.coli* BL21-CodonPlus(DE3)-RIL cells (Stratagene) and bound to Glutathione–Sepharose beads (20 μl; Amersham Biosciences) and chitin beads (20 μl; NEB), respectively, in NET-T150 buffer [10 mM Tris (pH 8.0), 1 mM EDTA, 150 mM NaCl and 0.1% (v/v) Triton X-100]. The beads were incubated with recombinant PCNA (0.5–2 μg) in 400 μl of NET-T150 buffer supplemented with ethidium bromide (50 μg/ml) for 2 h at 4°C. Bound proteins were analyzed by western blotting.

RESULTS

RECQ5β promotes strand exchange on synthetic DNA structures mimicking a stalled replication fork

To investigate whether the RECQ5β helicase is capable of promoting replication fork regression, we examined its activity on oligonucleotide-based forked structures with homologous arms, which had a 5 nt region of heterology adjacent to the three-way junction to prevent spontaneous branch migration. First, we prepared a partial forked duplex lacking the leading strand (3′-flap duplex) by RECQ5β-mediated annealing of a 60mer oligonucleotide representing the leading-strand template to a 3′-tailed duplex composed of a 30mer oligonucleotide and a ^{32}P-labeled 60mer oligonucleotide representing the lagging strand and the corresponding template strand, respectively (Figure 1A). This resulted in a rapid formation of the forked structure as detected by electrophoresis in non-denaturing polyacrylamide gel followed by phosphorimaging (Figure 1B, lanes 2–8). A small amount of the 60mer duplex was also detected, which had presumably arisen from spontaneous branch migration. Remarkably, upon the addition of ATP to this mixture, a robust strand-exchange activity was observed, resulting in the formation of the ^{32}P-labeled 60mer duplex (Figure 1B and C, lanes 9–15). Note that this duplex contains a small bubble due to the short region of heterology at the junction (Figure 1A). When ATP was substituted with its poorly hydrolysable analogue ATPγS, no strand exchange was observed over the period of 32 min, confirming that the RECQ5β-mediated strand exchange is dependent on the helicase activity of the enzyme (Figure 1B and C, lanes 16–22).

Certain RecQ DNA helicases such as human RECQ1 (26) have been shown to be sensitive to free magnesium cations. Hence, we sought to determine the optimal Mg^{2+}:ATP ratio for RECQ5β-mediated strand exchange reaction. To do so, we varied Mg^{2+} concentration in the range from 0 to 10 mM keeping ATP at a fixed concentration of 2 mM. We found that the extent of RECQ5β-mediated strand exchange on the 3′-flap substrate increased with increasing Mg^{2+} concentration in a hyperbolic fashion, reaching maximal values at Mg^{2+}:ATP ratios between 3 and 5 (Figure 1D). These data indicated that RECQ5β requires a molar excess of Mg^{2+} over ATP for efficient strand exchange activity. Therefore, all further experiments were performed using 2 mM ATP and 10 mM $Mg(OAc)_2$.

Next we investigated whether RECQ5β can promote strand exchange if the forked structure contains both the lagging and the leading strands. To mimic the structure of a replication fork blocked by a lesion on the leading-strand template, the length of the leading strand was chosen to be 10 nt shorter than the length of the lagging strand. The DNA substrate was again assembled using the strand-annealing function of RECQ5β (Figure 2A). Upon the addition of ATP, a rapid accumulation of free ^{32}P-labeled leading oligonucleotide was observed in the initial stages of the reaction which was followed by its annealing to the lagging oligonucleotide as evidenced by an accumulation of the 20mer/30mer duplex in the later stage of the reaction (Figure 2B and 2C, lanes 9–15). This indicates that RECQ5β has the ability to promote the displacement of both arms of the fork and subsequent annealing of the displaced leading and lagging strands

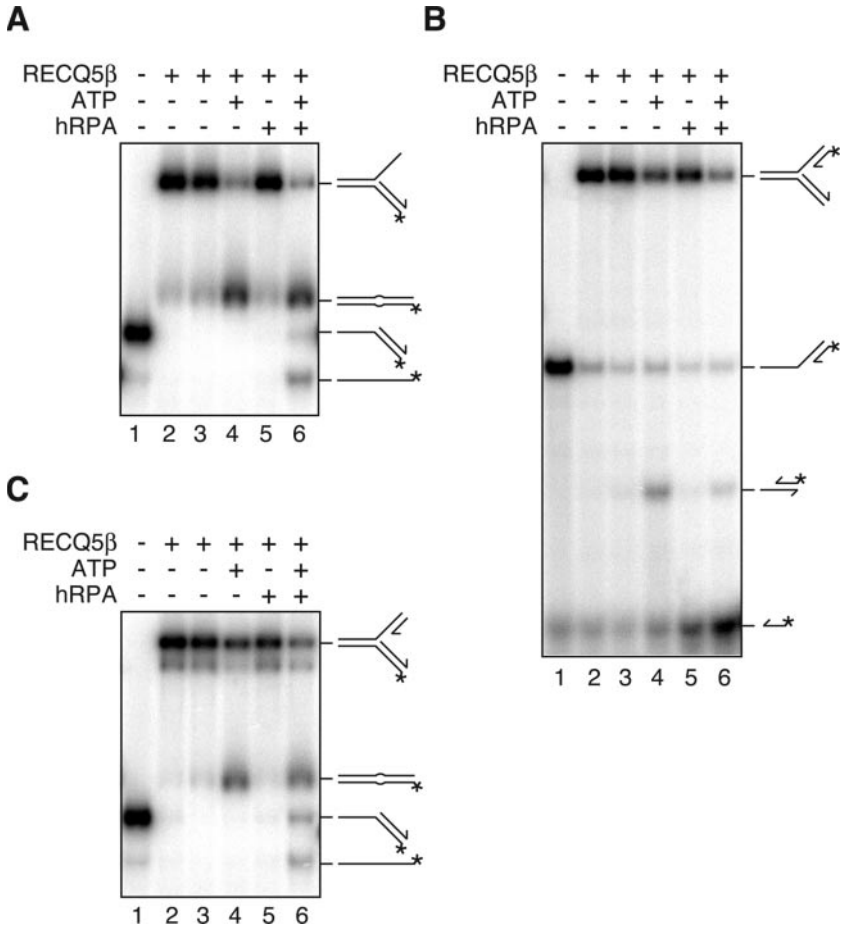

Figure 3. Effect of hRPA on RECQ5β-mediated strand exchange on forked DNA duplex lacking the leading strand (**A**) and forked DNA duplex with 10 nt leading-strand gap, radioactively labeled either on the leading-strand oligonucleotide (**B**) or on the lagging-strand template (**C**). The DNA substrates were prepared by RECQ5β mediated annealing as described in Materials and Methods and schematically indicated in Figures 1A and 2A. Reactions were carried out for 32 min as indicated. DNA, RECQ5β and hRPA were present at concentrations of 1, 40 and 20 nM, respectively. hRPA was added 2 min before the addition of ATP (2 mM).

(Figure 2B and C). No strand exchange was seen in the presence of ATPγS, indicating a requirement for the helicase activity of the enzyme (Figure 2B, lanes 16–22).

It is known that RPA covers single-stranded regions at stalled replication forks (27). Therefore, we investigated the effect of hRPA on the strand-exchange activity of RECQ5β using the synthetic forked structures described above. To monitor the annealing of the parental strands on the gapped fork structure, ^{32}P-label was also placed on the lagging-strand template. These experiments indicated that hRPA did not impair the RECQ5β-mediated annealing of the parental strands (Figure 3A and C). However, it was found to partially inhibit the annealing of the displaced leading and lagging oligonucleotides (Figure 3B). This is consistent with our earlier studies, which indicated that hRPA inhibits RECQ5β-mediated strand annealing (19). A partial shift of the reaction towards unwinding of the parental duplex was also observed, particularly with the gapped substrate (Figure 3C, compare lanes 4 and 6). However, this is not likely to be the consequence of binding of hRPA to the leading arm, since the single-strand gap on the gapped fork structure is too short (10 nt) to accommodate hRPA, assuming that the size of the DNA-binding site for RPA is ~30 nt (28).

Collectively, the findings described above suggested that RECQ5β is capable of promoting fork regression *in vitro*.

RPA blocks strand exchange by BLM and WRN

We also examined other human RecQ homologues, namely BLM and WRN, for the ability to promote strand exchange on the 3′-flap structure described above (Figure 1A). As WRN showed only negligible strand-annealing activity under the condition of our assay, the DNA substrate was prepared by spontaneous annealing of the constituent oligonucleotides, with the lagging oligonucleotide being present in a 5-fold molar excess over the parental strands. We found that both BLM and WRN could efficiently catalyze the conversion of the 3′-flap structure into the 60mer duplex (Figure 4A and B). However, if hRPA was present in the reaction, the action of both helicases was strongly biased toward unwinding of the parental duplex, as evidenced by the accumulation of the ^{32}P-labeled 30mer/60mer duplex in the course of the reaction (Figure 4C and D). In contrast, these time course experiments revealed that hRPA significantly stimulated the rate and the extent of RECQ5β-mediated strand exchange on 3′-flap structure (Figure 4).

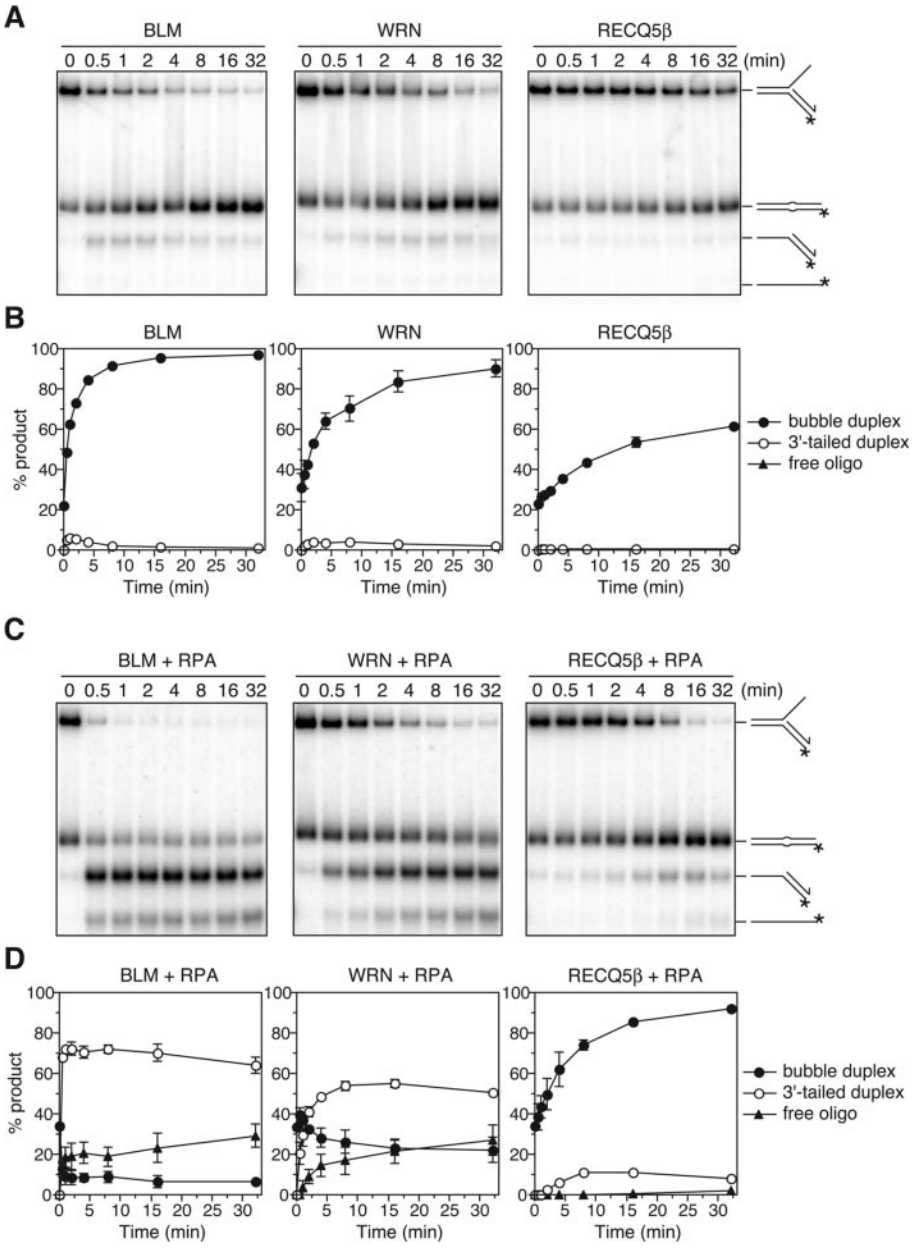

Figure 4. Strand exchange by BLM, WRN and RECQ5β in the absence and presence of hRPA. (**A**) Time course of reactions of 10 nM BLM, 5 nM WRN and 40 nM RECQ5β, respectively, with 1 nM forked DNA structure with homologous arms lacking the leading strand. (**B**) Quantification of reactions in (A). (**C**) Time course of reactions of 10 nM BLM, 5 nM WRN and 40 nM RECQ5β, respectively, with 1 nM DNA structure as in (A) in the presence of 20 nM hRPA. The DNA substrate was preincubated for 2 min with hRPA before addition of helicase. (**D**) Quantification of reactions in (C). The DNA substrate was the same as in Figure 1, except that it was prepared by spontaneous annealing of the component oligonucleotides as described in Materials and Methods. Reactions were analyzed as in Figure 1. In the graphs, relative concentrations of the products are plotted versus reaction time. The 60mer bubble duplex, filled circles; 3′-tailed 30mer/60mer duplex, open circles; free 60mer oligonucleotide, filled triangles. In all graphs, the data points represent the average values from three independent experiments.

These data indicate that there are mechanistic differences between RECQ5β and other human RecQ helicases in the mode of processing of forked DNA structures coated with hRPA.

RECQ5β actively unwinds only the lagging-strand arm of the fork

To gain insights into the mechanism of RECQ5β-mediated strand exchange, we investigated the action of RECQ5β on synthetic forked structures with heterologous arms to monitor only DNA unwinding events. In agreement with data reported for the *Drosophila* RECQ5 homologue (29), we found that on partial forked duplex lacking the leading strand (3′-flap duplex), RECQ5β showed preference for unwinding of the lagging-strand arm (Figure 5A and B). Interestingly, this reaction was significantly enhanced if the DNA substrate was pre-incubated with hRPA (compare Figure 5A and B). This could be the consequence of binding of hRPA to the single-stranded leading arm that would prevent loading of

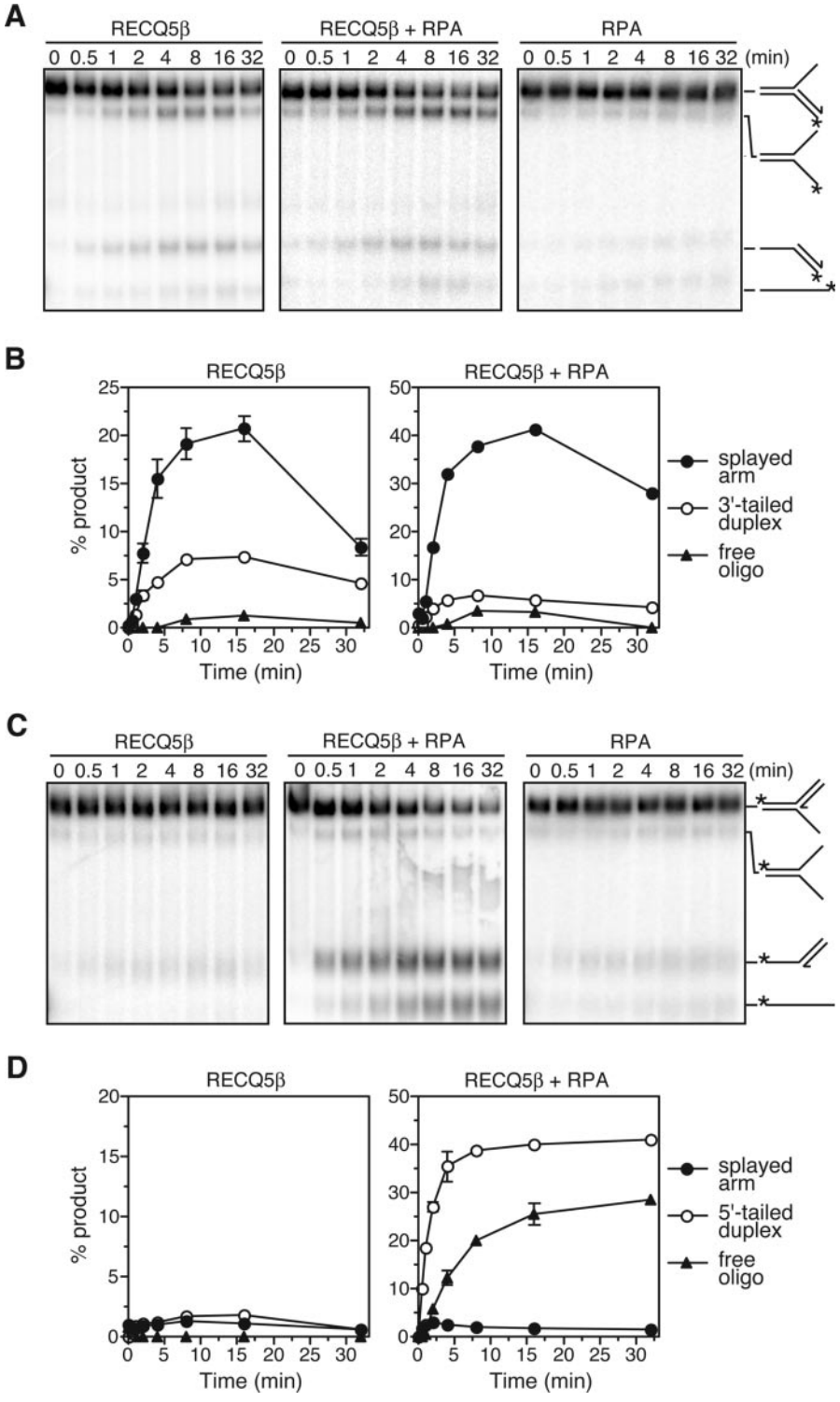

Figure 5. Unwinding of forked DNA structures with heterologous arms by RECQ5β. (**A**) Time course of RECQ5β-mediated unwinding of partial forked duplex lacking the leading strand (3′-flap duplex) in the absence and presence of 20 nM hRPA as indicated. Reaction containing RPA only is also shown as a control (**B**) Quantification of the RECQ5β-containing reactions in (A). The graph shows the relative concentrations of unwound products including the splayed arm (closed circles), the 3′-tailed duplex (open circles) and the free lagging-strand template (closed triangles). (**C**) Time course of RECQ5β-mediated unwinding of partial forked duplex lacking the lagging strand (5′-flap duplex) in the absence and presence of 20 nM hRPA. Reaction containing RPA only is also shown as a control (**D**) Quantification of the RECQ5β-containing reactions in (C). The graph shows the relative concentrations of unwound products including the splayed arm (closed circles) and the 3′-tailed duplex (open circles) and the free leading-strand template (closed triangles). All DNA substrates are derived from the same set of four oligonucleotides (RK1, RK2, RK5 and RK6) as described in Materials and Methods. The 3′ end of the leading and lagging strands are indicated by arrows. The position of the 5′-^{32}P label in each substrate is indicated by an asterisk. For all reactions, DNA substrates were present at a concentration of 1 nM. RECQ5β was 100 nM in the reactions without hRPA and 80 nM in the reactions with hRPA. Reactions were carried out and analyzed as described in Materials and Methods. In all graphs, the data points represent the average values from three independent experiments.

RECQ5β on this arm to initiate unwinding of the parental duplex. In agreement with this assumption, we found that hRPA inhibited RECQ5β-mediated unwinding of a 3′-tailed duplex if added to the DNA substrate prior to the helicase (data not shown). However, no significant stimulation of RECQ5β-mediated unwinding of the lagging-strand arm was observed with the *E.coli* single-stranded binding protein, indicating that this effect is specific for hRPA (Supplementary Figure S1).

To assess whether the RECQ5β helicase can actively unwind the leading arm of the fork, we examined its activity on partial forked duplex lacking the lagging strand (5′-flap duplex). We found that RECQ5β could catalyze only the unwinding of the parental arm on this structure, as evidenced by the accumulation of 5′-tailed duplex during the course of the reaction (Figure 5C and D). This was, however, seen only in the presence of hRPA, which is consistent with our previous finding that hRPA counteracts the intrinsic strand-annealing activity of RECQ5β (19). In the later stages of the hRPA-containing reaction, accumulation of the free leading oligonucleotide was also observed, which presumably resulted from a secondary unwinding event on the primary 5′-tail product. This observation is intriguing since the RECQ5β helicase was shown to exhibit a 3′–5′ polarity (19). It is possible that hRPA, if bound to the 5′-single stranded tail, can partially destabilize the duplex, which would allow loading of RECQ5β to mediate unwinding.

To further confirm that the RECQ5β helicase cannot actively remove the leading strand from the fork, we examined its action on a 5′-flap structure with homologous arms prepared from the same set of oligonucleotides as used in the previous strand exchange assays. If RECQ5β was capable of unwinding of the leading arm, it would promote strand exchange on this structure to form the 60mer duplex as it did on the homologous 3′-flap structure (Figure 1). However, RECQ5β did not show any strand-exchange activity on the 5′-flap structure, indicating that it cannot actively unwind the leading arm (Supplementary Figure S2).

We also examined the action of the BLM and WRN helicases on the forked DNA structures with heterologous arms described above. In contrast to RECQ5β, BLM and WRN displayed a strong preference for unwinding of the parental arm on all these structures, which was further enhanced by hRPA (Supplementary Figure S3). These findings are in agreement with previously published data (30) and further highlight mechanistic differences between RECQ5β and other human RecQ helicases in processing of forked DNA structures.

A domain within the non-conserved portion of RECQ5β is important for RECQ5β-mediated processing of forked DNA structures

To identify the functional domains in RECQ5β that are required for its ability to unwind the lagging arm of the fork and to promote strand exchange on forked structures in the presence of hRPA, we purified a series of truncated variants of RECQ5β lacking different parts of the region distal to the conserved helicase domain (Figure 6A). The RECQ5β variants lacking the C-terminal 266 or 340 amino acids ($RECQ5^{1–725}$ and $RECQ5^{1–651}$) were found to be proficient in promoting strand exchange on hRPA-coated forked structure lacking the leading strand albeit with a reduced efficiency compared to the wild-type enzyme (Figure 6B). Moreover, these variants retained the capacity to preferentially unwind the lagging-strand duplex on the forked structure with heterologous arms, being even more efficient than the wild-type enzyme (Figure 6D). This correlates with the fact that these mutants were severely impaired in promoting strand annealing (Figure 6C). In contrast, the $RECQ5^{1–475}$ and $RECQ5^{1–561}$ mutants were defective in promoting strand exchange and unwinding of the lagging arm (Figure 6B and D). However, these mutants could catalyze unwinding of the parental arm on the partial forked duplex lacking the leading strand, indicating that they retained the capacity to initiate duplex unwinding from a single-stranded tail (Figure 6D).

Collectively, these data indicate that the region of RECQ5β spanning the amino acids 561–651 is important for the processing of forked structures by this helicase.

RECQ5β is localized in DNA replication factories and persists at sites of stalled replication forks

To explore whether RECQ5β acts at DNA replications forks *in vivo*, we investigated its subcellular localization by immunofluorescence microscopy relative to PCNA that is widely used as a marker for DNA replication foci. It is known that PCNA foci undergo reproducible changes throughout S phase, with a fine punctuate pattern in early S, perinuclear and perinucleolar patterns in mid S and a characteristic late-S pattern with a few, but large foci (31). To monitor the RECQ5β localization pattern during S phase, we synchronized HeLa cells at the G_1/S transition by HU treatment and fixed them with methanol at different time points after release from the arrest. In addition to immunostaining, the cells were subjected to flow cytometry to determine the cell cycle distribution at individual time points. We observed that in HU-arrested cells, both PCNA and RECQ5β displayed exclusively nuclear staining, forming a large number of foci that partially co-localized (Figure 7). Three hours after the removal of HU (early S phase), >80% of PCNA foci in a single nucleus co-localized with RECQ5β foci in the majority of cells (Figure 7). Six hours after release (mid-S phase), the PCNA foci exhibited the characteristic peripheral pattern, while the RECQ5β foci were dispersed throughout the nucleus (Figure 7). Nine hours after release (late S phase), both PCNA and RECQ5β formed a few large foci that almost completely co-localized (Figure 7). We also examined the spatial distribution of RECQ5β and PCNA during S phase of U2OS osteosarcoma cells and obtained essentially the same results as in HeLa cells (Supplementary Figure S4). Moreover, in synchronized U2OS cells, the RECQ5β foci co-localized with sites of BrdU incorporation, a marker of ongoing DNA synthesis (Supplementary Figure S4). Using U2OS cells, we also found that the RECQ5β foci in late S phase co-localized with promyelocytic leukemia protein (PML), indicating that RECQ5β associates with PML nuclear bodies in this stage of the cell cycle (Supplementary Figure S5).

Next we investigated the effect of exogenously induced replication-blocking lesions on the cellular localization pattern of RECQ5β in non-synchronized HeLa cells. To induce

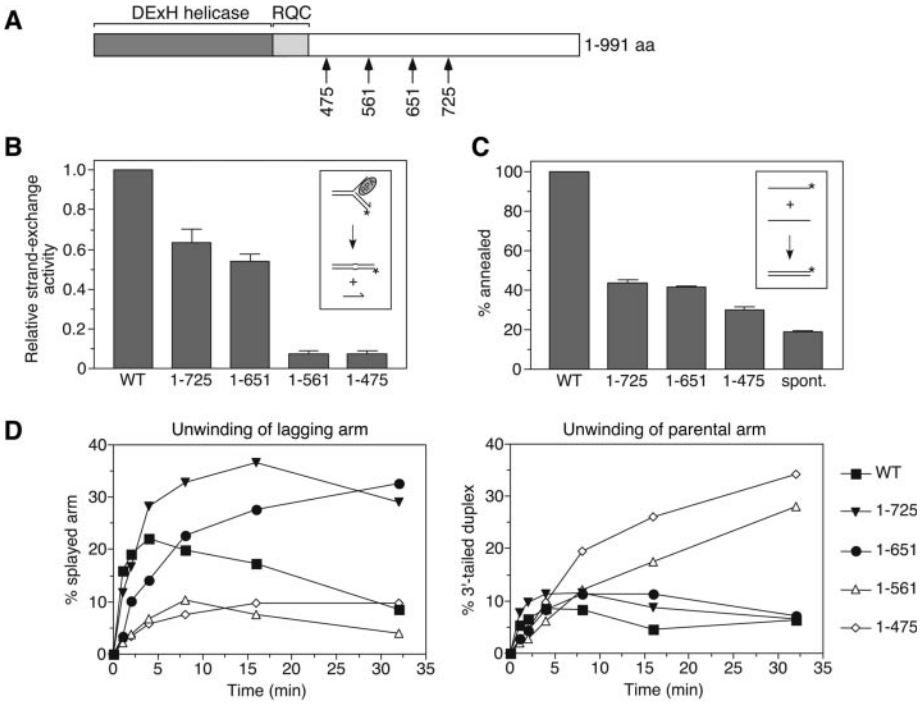

Figure 6. Characterization of RECQ5β mutants. (**A**) A schematic representation of the human RECQ5β protein demonstrating the location of the DExH helicase (dark gray) and RecQ C-terminal (RQC) (light gray) regions conserved among RecQ helicases. The arrowheads indicate the positions of the C-terminal ends of the truncated RECQ5β polypeptides used in this study. The numbers refer to the amino acid sequence of RECQ5β. (**B**) Comparison of strand-exchange activities of RECQ5β and its deletion variants (40 nM each) on forked DNA structure lacking the leading strand (1 nM) pre-coated with hRPA (20 nM). The reactions were incubated for 32 min and analyzed as described in Materials and Methods. Relative concentration of the 60mer duplex product was calculated for each reaction, and the values obtained were corrected by subtracting the background value (reaction without protein). Strand exchange activity of the mutants is expressed as a fraction of the wild-type activity. The inset shows the scheme of the reaction. (**C**) Annealing of 50mer complementary oligonucleotides, each at a concentration of 1 nM, in the presence of 20 nM wild-type and mutant RECQ5β proteins as indicated. Reactions were incubated for 32 min and the relative concentration of the strand-annealing product was determined as described in Materials and Methods. Values determined for spontaneous (spont.) reaction are also plotted. The inset shows the scheme of the reaction. (**D**) Kinetics of unwinding of 1 nM forked structure lacking the leading strand by 100 nM RECQ5β and its deletion variants as indicated. Reactions were carried out and analyzed as described in Materials and Methods. The graph on the left shows relative concentrations of splayed arm product resulting from unwinding of the lagging arm. The graph on the right shows relative concentration of the 3′-tailed duplex generated by unwinding of the parental arm. All data points represent the average values from three independent experiments.

the formation of bulky DNA adducts, cells were exposed to UVC irradiation or treated with CDDP. In asynchronous populations of cycling HeLa cells (~70% of cells in G_1 as judged from the FACS profile), PCNA showed mostly a diffuse nuclear staining, whereas RECQ5β displayed rather a punctuate distribution in the nucleus as well as a weak cytoplasmic staining (Figure 8). In a small percentage of cells (~15%), PCNA was concentrated in small nuclear foci, indicating that these cells were in S phase (data not shown). Most importantly, these PCNA foci largely co-localized with RECQ5β foci, which excludes the possibility that the pattern observed 3 h after HU removal was a consequence of DNA damage caused by HU treatment (data not shown; Figure 7).

After exposure of cells to UV irradiation at a dosage of 20 J/m^2, there was a dramatic increase in the percentage of cells in which PCNA foci co-localized with RECQ5β foci (Figure 8). Four hours after UV irradiation, ~80% of PCNA foci in a single nucleus co-localized with RECQ5β foci in 55% of cells. These foci appeared somewhat brighter than those observed in early S phase cells (compare Figure 7 and Figure 8) and persisted up to 6 h after irradiation (data not shown).

In HeLa cells treated with CDDP (20 μM), which predominantly causes intra-strand DNA cross-links mimicking pyrimidine–dimer adducts induced by UV light, RECQ5β and PCNA displayed essentially the same spatial distribution as in UV-irradiated cells, with the maximal co-localization being apparent 6 h after addition of the drug (Figure 8). Moreover, we examined spatial distribution of RECQ5β in SV40-immortalized human fibroblasts GM00637 and XP20SSV (XPA-deficient) before and after UV irradiation. We observed essentially the same patterns as in HeLa cells, excluding a cell-line specific effect (Supplementary Figure S6). In addition, the experiment with XPA-deficient cells ruled out the possibility that RECQ5β is present in the complexes that mediate repair synthesis following excision of DNA adducts by the nucleotide-excision repair pathway.

Taken together, these data suggest that RECQ5β is associated with the DNA replication machinery, particularly in early and late S phase and it is present in replication-repair factories at the sites of stalled replication forks.

RECQ5β directly interacts with PCNA

In addition to serving as a sliding clamp required for processive DNA synthesis, PCNA provides attachment sites for various other proteins that function in DNA replication, DNA repair, cell cycle progression and chromatin assembly

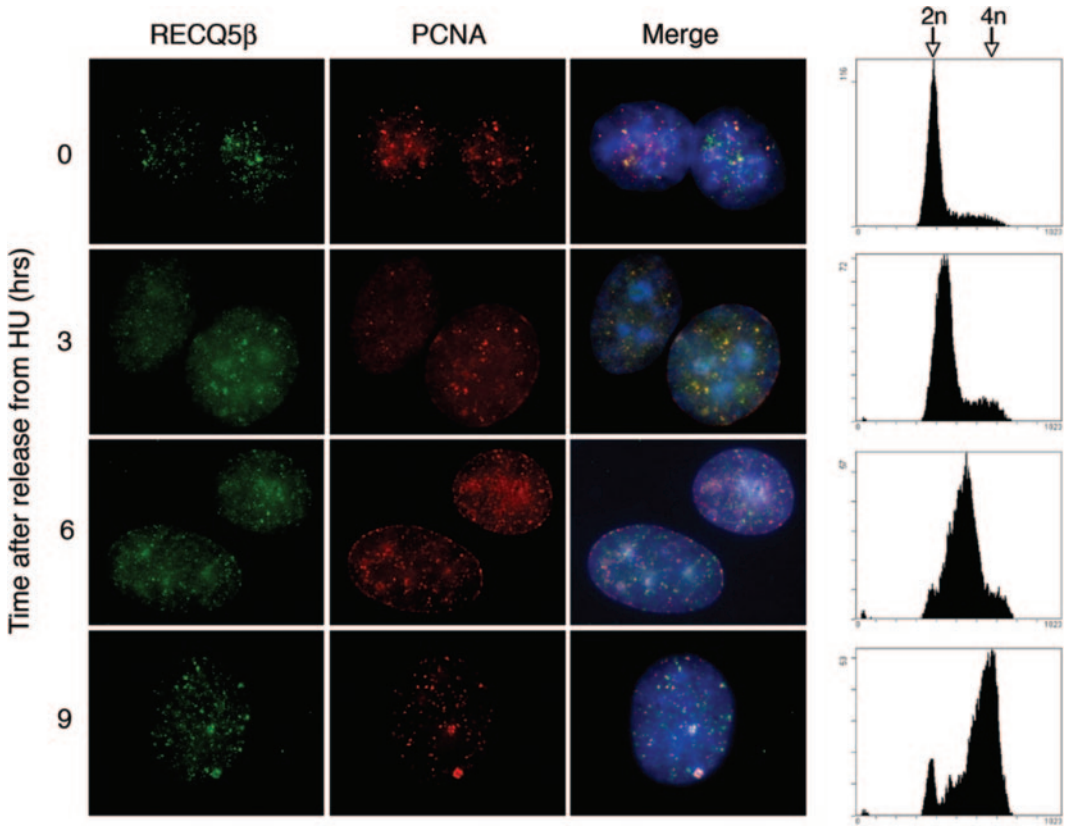

Figure 7. Co-localization of RECQ5β and PCNA in S phase nuclei of HeLa cells. Cells were synchronized at G_1/S transition by treatment with hydroxyurea (HU) for 16 h and then released to S phase by adding fresh medium without HU. At indicated time points, cells were fixed with methanol, triply stained for RECQ5β (green), PCNA (red) and DNA (blue) as described in Materials and Methods, and analyzed by fluorescence microscopy. Representative images are shown. Yellow colour in the superimposed images (Merge) indicates co-localization of RECQ5β and PCNA staining. In parallel, cells were subjected to FACS analysis. The resultant cell cycle profiles for each time point are shown on the right. Arrowheads indicate cell population in G_1 phase with a 2n DNA content and G_2/M with 4n DNA content; S phase cells have DNA content between 2n and 4n.

(32). To further explore the association of RECQ5β with the DNA replication machinery, we examined whether it interacts with PCNA, as suggested by the presence of a putative PCNA-binding motif at the C-terminus of RECQ5β (Figure 9A). First, we performed affinity pull-down assays with recombinant proteins produced in *E.coli*. We found that PCNA was bound to chitin beads coated with RECQ5β-CBD protein, but not to beads coated with McrA-CBD protein, indicating that the interaction was specific (Figure 9B). Moreover, using GST-tagged RECQ5β deletion variants, we found that the region spanning the last 200 amino acids of RECQ5β is essential for its interaction with PCNA, suggesting that this interaction is mediated through the putative PCNA-binding motif located in this region (Figure 9C).

We also examined the effect of PCNA on the strand exchange activity of RECQ5β using the synthetic forked DNA structure containing a 10 nt gap on the leading arm (Figure 2A). We found that PCNA did not affect the rate or the extent of RECQ5β-mediated strand exchange (Supplementary Figure S7).

To see whether RECQ5β interacts with PCNA *in vivo*, we conducted immunoprecipitation experiments with total extracts of human 293T embryonic kidney cells. Extracts were prepared not only from non-treated cells, but also from cells synchronized in early S phase and cells subjected to UV irradiation or CDDP treatment, since under these conditions, RECQ5β was found to localize to PCNA foci. We found that PCNA was precipitated with the anti-RECQ5β antibody, but not with control IgGs purified from pre-immune serum, indicating that RECQ5β and PCNA indeed form a complex *in vivo* (Figure 9D). Moreover, a significant larger amount of PCNA (~2 times) was detected in the immunoprecipitates of treated cells compared with non-treated cells, suggesting that the observed recruitment of RECQ5β to replication foci may occur via a direct interaction with PCNA (Figure 9D, compare lane 3 to lanes 4–6).

DISCUSSION

There is growing evidence suggesting that RecQ DNA helicases operate in various DNA repair processes induced by DNA replication defects. However, the DNA transactions mediated by these proteins at damaged replication forks still remain elusive. Here we show that the human RECQ5β helicase possesses the ability to promote strand exchange on synthetic forked DNA structures that mimic a stalled replication fork. Moreover, we provide evidence suggesting that the RECQ5β protein is localized in the DNA replication factories

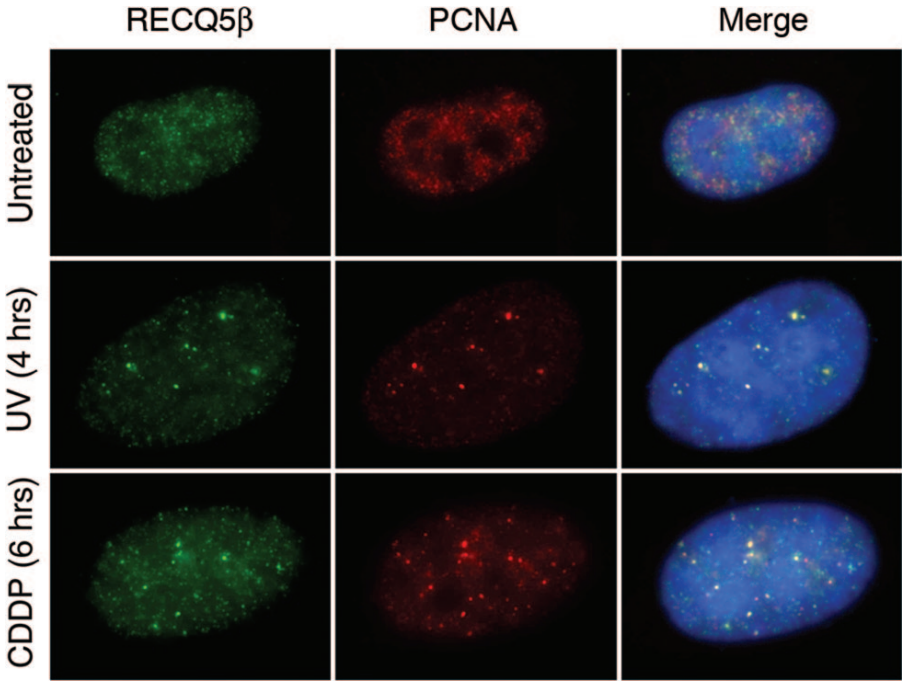

Figure 8. Co-localization of RECQ5β and PCNA in HeLa cells following UV irradiation and CDDP treatment. Non-synchronized cells were UV-irradiated at 20 J/m^2 and cultured for additional 4 h or treated with 20 μM CDDP for 6 h. After methanol fixation, cells were triply stained for RECQ5β (green), PCNA (red) and DNA (blue), and analyzed by fluorescence microscopy. Representative images are shown.

in S phase nuclei and persists at the sites of stalled replication forks. Based on these findings, we speculate that the RECQ5β helicase could mediate regression of stalled replication forks *in vivo* to facilitate DNA damage bypass by template-switching (Supplementary Figure S8). As mentioned above, such a DNA damage tolerance mechanism has been postulated to exist in both prokaryotic and eukaryotic organisms, but remains to be substantiated experimentally. In the budding yeast *Saccharomyces cerevisiae*, fork regression associated with template-switching is thought to be the underlying mechanism of the *RAD5*-subpathway of *RAD6*-dependent postreplicative repair, which is highly conserved from yeast to humans (33). As this DNA damage tolerance process, which involves non-destructive polyubiquitination of PCNA, is largely independent of the HR machinery, other means, such as helicase-promoted DNA unwinding, would be required to accomplish the strand-exchange events required for fork regression (33,34). At present, however, it is not clear whether Sgs1 helicase, the sole RecQ homologue in *S.cerevisiae*, is involved in the RAD6-dependent DNA damage tolerance, since the assessment of this possibility by epistatic analysis is complicated due to the involvement of Sgs1 in the HR pathway of postreplicative repair (6). Nevertheless, some evidence for such a function has been provided in the fission yeast *Saccharomyces pombe* by the observation that the formation of Rqh1 (Sgs1 homologue) foci upon UV irradiation is dependent on the presence of Rdh18/Rad18, a component of the Rad6 pathway (35).

Our hypothesis that RECQ5β operates in the repair of damaged replication forks is consistent with the finding that inactivation of the mouse RECQ5β homologue is associated with a significant increase in the frequency of SCEs (17), as these may represent cross-over outcomes of the HR-mediated repair of broken replication forks that arise as a consequence of the blockage of leading-strand extension by bulky lesions (Supplementary Figure S8). Similarly, elevated SCE levels have been observed in DT40 chicken cells lacking the trans-lesion polymerases Polζ and Polκ, or the Rad18 ubiquitin ligase (36). However, one cannot exclude the possibility that the increased level of mitotic recombination associated with RECQ5β deficiency results from a defect in another DNA repair mechanisms. For example, RECQ5β could operate in the synthesis-dependent strand-annealing pathway of DNA double-strand break repair by disrupting D-loops and promoting annealing of extended arms of the broken chromosome. Alternatively, RECQ5β could suppress unscheduled recombination during DNA replication by directly displacing inappropriately formed RAD51 filaments in the same manner as the Srs2 and UvrD helicases (37,38).

The biochemical and structural studies have revealed that the *E.coli* RecG helicase mediates fork regression by active unwinding of both the leading and lagging arms of the fork using a wedge domain that is simultaneously pushed into the lagging and the leading duplexes promoting strand displacement (39,40). In contrast to RecG, the RECQ5β helicase was found to unwind only the lagging-strand duplex, which raises the question of how it can promote fork regression beyond the leading-strand gap. We propose a mechanism in which RECQ5β binds to the fork junction and subsequently translocates along the lagging-strand template in the 3′–5′ direction to unwind the lagging-strand duplex. As a result, the parental strands will be free to re-anneal. Interestingly, we identified a region of 90 amino acids, located within the non-conserved portion of RECQ5β, as being required for its ability to unwind the lagging arm of the fork, but not for RECQ5β-mediated unwinding of 3′-tailed DNA duplexes.

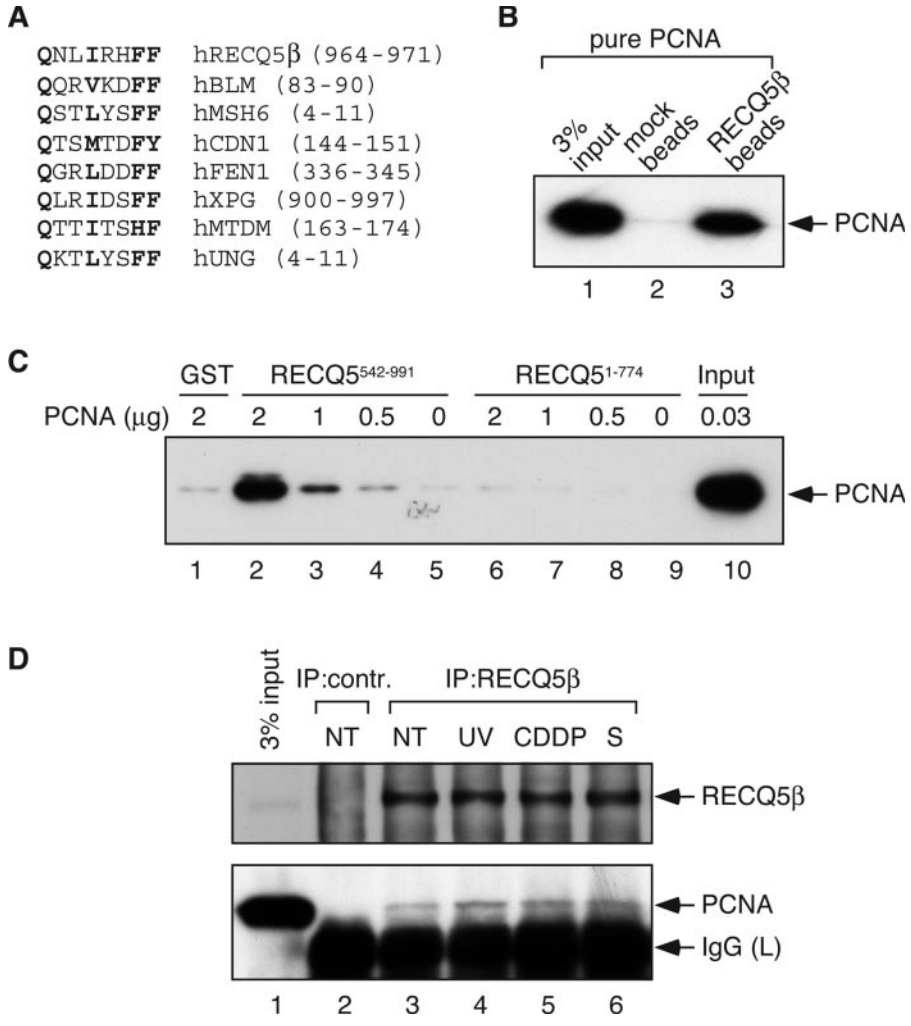

Figure 9. Interaction between RECQ5β and PCNA. (**A**) The putative PCNA-binding motif of human RECQ5β. The C-terminal amino acids 964–971 of RECQ5β are aligned with the PCNA-binding motifs identified in various PCNA-interacting proteins. The highly conserved residues are shown in boldface. (**B**) Direct interaction between RECQ5β and PCNA. Chitin beads coated with recombinant RECQ5β protein containing an intein-CBD tag were incubated with recombinant PCNA (1 μg) as described in Materials and Methods. In the control experiment, beads coated with the *E.coli* McrA endonuclease (mock beads) were used. Bound proteins were analyzed by SDS–PAGE and western blotting. Blots were probed with monoclonal anti-PCNA antibody (PC-10, Santa Cruz). (**C**) Mapping PCNA-interaction domain in RECQ5β. Glutathione beads coated with the GST-tagged RECQ5β deletion variants $RECQ5^{542–991}$ and $RECQ5^{1–774}$, respectively, were incubated with increasing amounts of purified PCNA as indicated. Bound proteins were analyzed as in (B). (**D**) Co-immunoprecipitation of PCNA with RECQ5β from extracts of 293T cells: non-treated (NT) cells (lane 3), UV-irradiated (40 J/m^2) cells incubated for 6 h (lane 4), cells treated with CDDP (20 μM) for 8 h (lane 5), cells arrested at G_1/S by HU (2 mM, 16 h) and subsequently released to S phase for 3 h (lane 6). Extracts were immunoprecipitated using affinity-purified rabbit polyclonal anti-RECQ5β antibody as described in Materials and Methods. IgGs purified from corresponding pre-immune serum served as a control (lane 2). The immunoprecipitates were analyzed as in (A). The blots were probed with anti-PCNA and anti-RECQ5β antibodies.

It is therefore plausible to propose that this domain may govern the loading of the RECQ5β helicase on the fork junction, placing the helicase motor on the parental duplex in such an orientation as to allow translocation towards the lagging arm. Furthermore, we propose that when the moving junction encounters the leading strand, spontaneous strand exchange will take place, resulting in the displacement of the leading strand and its annealing to the displaced lagging strand to form a four-way junction. This reaction will be favoured due to the concomitant unwinding of the lagging arm by RECQ5β. It is also possible that the annealing events occurring during the fork regression process are promoted by the C-terminal strand-annealing domain of RECQ5β, since we found that the deletion variants $RECQ5^{1–725}$ and $RECQ5^{1–651}$ were dramatically compromised for the strand-annealing activity and showed reduced strand-exchange activity relative to the wild-type protein.

A previous study demonstrated that BLM and WRN have the capacity to promote strand exchange on oligonucleotide-based substrates through combining their strand-pairing and helicase activities (41). More recently, the BLM helicase has been found to promote fork regression on plasmid-sized substrates, generating a four-way structure (42). Interestingly, we found that hRPA, which covers single-stranded regions at stalled forks (27), strongly modulated the action of the BLM and WRN helicases at the fork to favour unwinding of the parental duplex, which is consistent with the previous reports demonstrating that hRPA increases the processivity of the

BLM and WRN helicases through direct protein–protein interactions (43,44). However, these experiments using short DNA substrates cannot account for the possibility that fork regression is mediated by another helicase molecule loaded on the liberated lagging-strand template, an model proposed for the *E.coli* RecQ helicase (45). To assess which human RecQ helicase is more likely to promote fork regression *in vivo*, the effect of hRPA on fork regression by BLM, WRN and RECQ5β is currently being investigated using a plasmid-sized forked DNA structure containing an extensive leading-strand gap.

SUPPLEMENTARY DATA

Supplementary Data are available at NAR Online.

ACKNOWLEDGEMENTS

We thank Nina Mojas for help in fluorescence microscopy, Christiane Koenig for technical assistance and Josef Jiricny, Massimo Lopes and Ludovic Gillet for comments on the manuscript. This work was funded by the Swiss National Science Foundation and the Sassella Stiftung. Funding to pay the Open Access publication charges for this article was provided by the Swiss National Science Foundation.

Conflict of interest statement. None declared.

REFERENCES

1. Cox,M.M. (2001) Recombinational DNA repair of damaged replication forks in *Escherichia coli*: questions. *Annu. Rev. Genet.*, **35**, 53–82.
2. Cordeiro-Stone,M., Makhov,A.M., Zaritskaya,L.S. and Griffith,J.D. (1999) Analysis of DNA replication forks encountering a pyrimidine dimer in the template to the leading strand. *J. Mol. Biol.*, **289**, 1207–1218.
3. Lopes,M., Foiani,M. and Sogo,J.M. (2006) Multiple mechanisms control chromosome integrity after replication fork uncoupling and restart at irreparable UV lesions. *Mol. Cell*, **21**, 15–27.
4. Hickson,I.D. (2003) RecQ helicases: caretakers of the genome. *Nat. Rev. Cancer*, **3**, 169–178.
5. Lambert,S., Watson,A., Sheedy,D.M., Martin,B. and Carr,A.M. (2005) Gross chromosomal rearrangements and elevated recombination at an inducible site-specific replication fork barrier. *Cell*, **121**, 689–702.
6. Barbour,L. and Xiao,W. (2003) Regulation of alternative replication bypass pathways at stalled replication forks and its effects on genome stability: a yeast model. *Mutat. Res.*, **532**, 137–155.
7. Heller,R.C. and Marians,K.J. (2006) Replication fork reactivation downstream of a blocked nascent leading strand. *Nature*, **439**, 557–562.
8. Higgins,N.P., Kato,K. and Strauss,B. (1976) A model for replication repair in mammalian cells. *J. Mol. Biol.*, **101**, 417–425.
9. Seigneur,M., Bidnenko,V., Ehrlich,S.D. and Michel,B. (1998) RuvAB acts at arrested replication forks. *Cell*, **95**, 419–430.
10. Zou,H. and Rothstein,R. (1997) Holliday junctions accumulate in replication mutants via a RecA homolog-independent mechanism. *Cell*, **90**, 87–96.
11. Sogo,J.M., Lopes,M. and Foiani,M. (2002) Fork reversal and ssDNA accumulation at stalled replication forks owing to checkpoint defects. *Science*, **297**, 599–602.
12. Bachrati,C.Z. and Hickson,I.D. (2003) RecQ helicases: suppressors of tumorigenesis and premature aging. *Biochem. J.*, **374**, 577–606.
13. Wu,L. and Hickson,I.D. (2003) The Bloom's syndrome helicase suppresses crossing over during homologous recombination. *Nature*, **426**, 870–874.
14. Crabbe,L., Verdun,R.E., Haggblom,C.I. and Karlseder,J. (2004) Defective telomere lagging strand synthesis in cells lacking WRN helicase activity. *Science*, **306**, 1951–1953.
15. Opresko,P.L., Otterlei,M., Graakjaer,J., Bruheim,P., Dawut,L., Kolvraa,S., May,A., Seidman,M.M. and Bohr,V.A. (2004) The Werner syndrome helicase and exonuclease cooperate to resolve telomeric D loops in a manner regulated by TRF1 and TRF2. *Mol. Cell*, **14**, 763–774.
16. Sangrithi,M.N., Bernal,J.A., Madine,M., Philpott,A., Lee,J., Dunphy,W.G. and Venkitaraman,A.R. (2005) Initiation of DNA replication requires the RECQL4 protein mutated in Rothmund-Thomson syndrome. *Cell*, **121**, 887–898.
17. Hu,Y., Lu,X., Barnes,E., Yan,M., Lou,H. and Luo,G. (2005) Recql5 and Blm RecQ DNA helicases have nonredundant roles in suppressing crossovers. *Mol. Cell. Biol.*, **25**, 3431–3442.
18. Shimamoto,A., Nishikawa,K., Kitao,S. and Furuichi,Y. (2000) Human RecQ5β, a large isomer of RecQ5 DNA helicase, localizes in the nucleoplasm and interacts with topoisomerases 3α and 3β. *Nucleic Acids Res.*, **28**, 1647–1655.
19. Garcia,P.L., Liu,Y., Jiricny,J., West,S.C. and Janscak,P. (2004) Human RECQ5β, a protein with DNA helicase and strand-annealing activities in a single polypeptide. *EMBO J.*, **23**, 2882–2891.
20. Gaymes,T.J., North,P.S., Brady,N., Hickson,I.D., Mufti,G.J. and Rassool,F.V. (2002) Increased error-prone non homologous DNA end-joining—a proposed mechanism of chromosomal instability in Bloom's syndrome. *Oncogene*, **21**, 2525–2533.
21. Karow,J.K., Chakraverty,R.K. and Hickson,I.D. (1997) The Bloom's syndrome gene product is a 3′–5′ DNA helicase. *J. Biol. Chem.*, **272**, 30611–30614.
22. Orren,D.K., Brosh,R.M., Jr., Nehlin,J.O., Machwe,A., Gray,M.D. and Bohr,V.A. (1999) Enzymatic and DNA binding properties of purified WRN protein: high affinity binding to single-stranded DNA but not to DNA damage induced by 4NQO. *Nucleic Acids Res.*, **27**, 3557–3566.
23. Henricksen,L.A., Umbricht,C.B. and Wold,M.S. (1994) Recombinant replication protein A: expression, complex formation, and functional characterization. *J. Biol. Chem.*, **269**, 11121–11132.
24. Podust,L.M., Podust,V.N., Sogo,J.M. and Hubscher,U. (1995) Mammalian DNA polymerase auxiliary proteins: analysis of replication factor C-catalyzed proliferating cell nuclear antigen loading onto circular double-stranded DNA. *Mol. Cell. Biol.*, **15**, 3072–3081.
25. Janscak,P., Garcia,P.L., Hamburger,F., Makuta,Y., Shiraishi,K., Imai,Y., Ikeda,H. and Bickle,T.A. (2003) Characterization and mutational analysis of the RecQ core of the Bloom syndrome protein. *J. Mol. Biol.*, **330**, 29–42.
26. Sharma,S., Sommers,J.A., Choudhary,S., Faulkner,J.K., Cui,S., Andreoli,L., Muzzolini,L., Vindigni,A. and Brosh,R.M., Jr. (2005) Biochemical analysis of the DNA unwinding and strand annealing activities catalyzed by human RECQ1. *J. Biol. Chem.*, **280**, 28072–28084.
27. Zou,L. and Elledge,S.J. (2003) Sensing DNA damage through ATRIP recognition of RPA-ssDNA complexes. *Science*, **300**, 1542–1548.
28. Kim,C., Snyder,R.O. and Wold,M.S. (1992) Binding properties of replication protein A from human and yeast cells. *Mol. Cell. Biol.*, **12**, 3050–3059.
29. Ozsoy,A.Z., Ragonese,H.M. and Matson,S.W. (2003) Analysis of helicase activity and substrate specificity of Drosophila RECQ5. *Nucleic Acids Res.*, **31**, 1554–1564.
30. Brosh,R.M., Jr., Waheed,J. and Sommers,J.A. (2002) Biochemical characterization of the DNA substrate specificity of Werner syndrome helicase. *J. Biol. Chem.*, **275**, 23500–23508.
31. Leonhardt,H., Rahn,H.P., Weinzierl,P., Sporbert,A., Cremer,T., Zink,D. and Cardoso,M.C. (2000) Dynamics of DNA replication factories in living cells. *J. Cell. Biol.*, **149**, 271–280.
32. Warbrick,E. (2000) The puzzle of PCNA's many partners. *Bioessays*, **22**, 997–1006.
33. Torres-Ramos,C.A., Prakash,S. and Prakash,L. (2002) Requirement of *RAD5* and *MMS2* for postreplication repair of UV-damaged DNA in *Saccharomyces cerevisiae*. *Mol. Cell. Biol.*, **22**, 2419–2426.
34. Hoege,C., Pfander,B., Moldovan,G.L., Pyrowolakis,G. and Jentsch,S. (2002) RAD6-dependent DNA repair is linked to modification of PCNA by ubiquitin and SUMO. *Nature*, **419**, 135–141.
35. Laursen,L.V., Ampatzidou,E., Andersen,A.H. and Murray,J.M. (2003) Role for the fission yeast RecQ helicase in DNA repair in G2. *Mol. Cell. Biol.*, **23**, 3692–3705.

36. Hochegger,H., Sonoda,E. and Takeda,S. (2004) Post-replication repair in DT40 cells: translesion polymerases versus recombinases. *Bioessays*, **26**, 151–158.
37. Krejci,L., Van Komen,S., Li,Y., Villemain,J., Reddy,M.S., Klein,H., Ellenberger,T. and Sung,P. (2003) DNA helicase Srs2 disrupts the Rad51 presynaptic filament. *Nature*, **423**, 305–309.
38. Veaute,X., Delmas,S., Selva,M., Jeusset,J., Le Cam,E., Matic,I., Fabre,F. and Petit,M.A. (2005) UvrD helicase, unlike Rep helicase, dismantles RecA nucleoprotein filaments in *Escherichia coli*. *EMBO J.*, **24**, 180–189.
39. McGlynn,P. and Lloyd,R.G. (2001) Rescue of stalled replication forks by RecG: simultaneous translocation on the leading and lagging strand templates supports an active DNA unwinding model of fork reversal and Holliday junction formation. *Proc. Natl Acad. Sci. USA*, **98**, 8227–8234.
40. Singleton,M.R., Scaife,S. and Wigley,D.B. (2001) Structural analysis of DNA replication fork reversal by RecG. *Cell*, **107**, 79–89.
41. Machwe,A., Xiao,L., Groden,J., Matson,S.W. and Orren,D.K. (2005) RecQ family members combine strand pairing and unwinding activities to catalyze strand exchange. *J. Biol. Chem.*, **280**, 23397–23407.
42. Ralf,C., Hickson,I.D. and Wu,L. (2006) The Bloom's syndrome helicase can promote the regression of a model replication fork. *J. Biol. Chem.*, **281**, 22839–22846.
43. Brosh,R.M., Jr., Li,J.L., Kenny,M.K., Karow,J.K., Cooper,M.P., Kureekattil,R.P., Hickson,I.D. and Bohr,V.A. (2000) Replication protein A physically interacts with the Bloom's syndrome protein and stimulates its helicase activity. *J. Biol. Chem.*, **275**, 23500–23508.
44. Brosh,R.M., Jr., Orren,D.K., Nehlin,J.O., Ravn,P.H., Kenny,M.K., Machwe,A. and Bohr,V.A. (1999) Functional and physical interaction between WRN helicase and human replication protein A. *J. Biol. Chem.*, **274**, 18341–18350.
45. Hishida,T., Han,Y.W., Shibata,T., Kubota,Y., Ishino,Y., Iwasaki,H. and Shinagawa,H. (2004) Role of the *Escherichia coli* RecQ DNA helicase in SOS signaling and genome stabilization at stalled replication forks. *Genes Dev.*, **18**, 1886–1897.